Sequence of Morphological Transitions in Two-Dimensional Pattern Growth from Aqueous Ascorbic Acid Solutions

A. S. Paranjpe

Solid State Physics Division, Bhabha Atomic Research Centre, Trombay, Mumbai 400 085, India

(Received 19 November 2001; published 29 July 2002)

A sequence of morphological transitions in two-dimensional dehydration patterns of aqueous solutions of ascorbic acid is observed with humidity as a control parameter. Change in morphology occurs due to humidity induced variation in the concentration of the metastable supersaturated solution phase formed after initial solvent evaporation. As percent humidity is varied from 40 to 80, patterns change from compact circular → radial → density modulated radial (a new morphology) → density modulated circular → density modulated dendritic (a new morphology) → dense branching.

DOI: 10.1103/PhysRevLett.89.075504 PACS numbers: 81.10.Dn, 68.55.Jk, 68.90.+g, 81.15.Lm

Pattern formation is a complex phenomenon occurring due to rich interplay between diverse forces such as viscosity and molecular diffusion, anisotropy in surface tension, external electric and magnetic fields, pressure, and temperature [1]. Added to these, pattern formation from aqueous solutions is also influenced by solution concentration, loss of water by evaporation, and convective forces [2,3]. In general, the study of morphological variations is undertaken with an aim to understand the mechanism of growth of a particular morphology and universality, if any, underlying the growth mechanism for similar morphologies observed in different systems. In most of the systems studied, some force field such as electric field [4], pressure [5], or magnetic field [6] is used to induce change in these parameters and, hence, for varying morphologies. In diffusion limited growths, in the absence of sufficient anisotropy, repeated tip splitting dominates the interfacial dynamics. This, in the presence of surface tension, gives rise to fractal structures [7–9]. Repeated tip splitting gives rise to dense branching morphology in the limit of vanishing effective surface tension [10]. Anisotropy plays an important role in dendritic growths [11].

I present here the first systematic experimental investigation of morphological transitions occurring in two-dimensional pattern growth during natural dehydration of a simple system of aqueous ascorbic acid solutions. The interesting observation that triggered these experiments is the apparent coexistence of morphologies at constant initial solution concentration, on the same substrate, and under thermal conditions. Coexistence of morphologies under isothermal conditions is thought to be due to velocity selection, fastest growing mode being selected [12,13]. However, in experimental growths, there should be some physical parameter such as diffusion constant, surface tension, or intermolecular interactions, a change in which induces morphological variation. A careful experimentation with the present system revealed that, by varying humidity, morphological transitions could be obtained in a controlled manner. Hence, it was thought that humidity must be changing a parameter, which is responsible for the change in morphology. A systematic study of the dehydrating film was undertaken to identify this parameter.

Some of the dehydration patterns reported here show density modulations along the growth direction (popularly known as ring morphologies). Ring morphologies, with different mechanisms of their formation, have been reported in several systems. For example, in freely suspended chiral smectic C liquid crystal films [14], ring patterns are formed in response to an in plane rotating electric field. Liesegang rings appear due to two moving reactant fronts with periodic removal of a weakly soluble reaction product [15]. Bacterial colony growths also show ring morphology [16]. In interfacial electrodeposition, ring morphology occurs due to oscillatory accumulation/detachment cycles of hydrogen generated at the growing edge of the deposits [17]. In the present system, patterns are grown in isotropic conditions, and instabilities related to direction dependent effects are absent. The mechanism of ring formation appears to be similar to that in dehydration patterns of aqueous solutions of glucose and sucrose [3].

Aqueous ascorbic acid solutions with $0.1M$ concentration were prepared by dissolving a requisite amount of solute in double distilled water at room temperature and filtered subsequently. 7.8×10^{-2} ml/cm^2 of the solutions were spread on precleaned glass slides. The thickness of the solution (0.078 cm) was very small compared to the linear dimension of the sample (2.5 cm), thus resulting in a nearly two-dimensional layer. The glass slides were mounted on leveled benches inside a constant temperature constant humidity bath (CTCHB). The bath temperature was maintained at $21.5 \pm 1\,^{\circ}$C. Percent humidity (H) was held constant for each set of experiments. For obtaining different morphologies, H was varied from about 40 to 80. The volume of the bath (64 L) $\gg$ sample volume (0.0005 L). Hence, spontaneous change in humidity due to solvent evaporation is negligible.

Solutions used in these experiments are very dilute, with starting concentration $c = 0.1M$ ($< 2\%$ by weight), so

that $c \ll c_s$, where c_s is the saturated solution concentration. Hence, it is not possible to get any precipitation from this solution. In a freely evaporating film such as this, there is a continuous loss of water and, at some stage, the solution concentration exceeds the saturation limit. At this stage, the system becomes unstable resulting in solute precipitation. The morphology of the pattern evolved depends upon supersaturated solution concentration (c_{ss}, in weight percent) which can change with the rate of evaporation. This is a normal scenario, for example, in dehydration of solutions of ionic salts such as NaCl, $CuSO_4$, $CuCl_2$, or $ZnSO_4$. The present system shows a very different behavior. Here, the solution attains a metastable state, where c_{ss} is very high and remains constant for a long period of time before the onset of nucleation and subsequent pattern growth. For a freely dehydrating film with $c = 0.1M$, Fig. 1 gives a plot of sample weight as a function of time at $H = 40$, 61, and 77. At $H = 77$, for about the first 15 hours, there is a steady reduction in the weight of the sample, $\sim 5.50 \times 10^{-4} \pm 8.59 \times 10^{-6}$ g/min. After about 15 h, loss of water is insignificant, the sample weight remaining almost constant hereafter. The solution is supersaturated with $c_{ss} \sim 75$. Thus, a metastable solution state is formed, where evaporation is almost negligible. c_{ss} depends upon temperature and humidity of the bath and, for $T = 21.5\,^{\circ}\mathrm{C}$, c_{ss} varies from about > 90 for $H = 40$ to about <75 for $H = 80$.

As is evidenced by constancy of solution concentration (right of point *a* in Fig. 1) and lack of nucleation for a long period of time, precipitation is difficult even when a supersaturated solution is formed. Nucleation occurs due to any instability, such as local fluctuation in concentration, temperature, or presence of an impurity. After nucleation occurs, a depletion region is formed around the precipitate with a concentration $c'_{ss} < c_{ss}$. The system, then, again tries to attain equilibrium by evaporation of water and subsequent attainment of steady state concentration c_{ss}. It is the competition between the rate of this evaporation, the rate of precipitation, the solution concentrations c_{ss} and c'_{ss}, and the interactions between solution, solute, solvent, and the substrate, which then decides the morphology of the subsequent pattern that evolves. At $H = 40$, nucleation sets in quite fast, about 2 h after the solution attains a steady concentration. However, as the humidity is increased further, although the steady concentration is reached in about 10 h, nucleation takes a longer time, a couple of days. For $H > 60$, it takes a couple of weeks for nucleation to occur. Once a nucleation center is formed, pattern growth is very fast and is completed in a couple of hours.

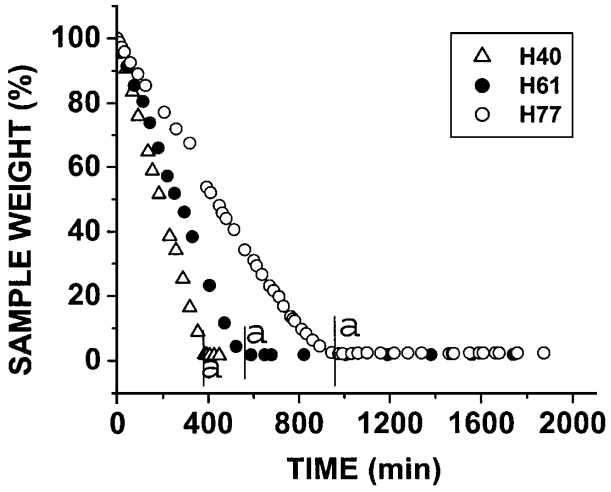

FIG. 1. Percent sample weight as a function of time for $H = 40$, 61, and 77.

The sequence of morphologies observed for different settings of humidity is seen in Fig. 2. Although observed morphology depends upon c_{ss}, H is used as a parameter. This is because H is read directly on the hygrometer whereas c_{ss} is estimated indirectly as it depends upon weights of the sample after supersaturation and after total dehydration, and it is difficult to measure its absolute value. The typical size of a fully grown pattern is about a centimeter or two and the different morphologies can be observed with the naked eye also. Microscopic observations are made under crossed polarizers so that the background is dark and the contrast improves. At $H = 40$, a compact circular (CC) growth is observed [Fig. 2(a)]. The deposition is spatially uniform. Above $H \sim 50$, the circular growth starts becoming radial with a circular envelope [Fig. 2(b)]. We call this a radial morphology (RM). For $H = 57$, density modulations along the radius start appearing, thus giving a density modulated radial (DMR) morphology [Fig. 2(c)]. With an increase in H to about 65 to 70, morphology changes to density modulated circular (DMC) morphology [Fig. 2(d)]. Here, the growth occurs on well-defined rings, and no specific structure is observed along the radius. For the above four morphologies, a spatial variation in intensity of light is observed indicating that there is preferential orientation of optic axes of microcrystallites. Around $H \sim 72$, morphology changes to a density modulated dendritic (DMD) [Fig. 2(e)]. The dendrites grow as if there is no break in their growth due to a change in density, which almost drops to zero at regular intervals. So, three ring morphologies are observed in this system. The differences between the three are as follows: In the DMR morphology, the fjords grow radially. There are no fjords observed for the DMC morphology; the average density is distributed on rings. Density modulated dendrites show a fluctuation in the direction of growth of fjords and a variation in density along the radius. As the humidity is increased further for $H \sim 80$, the morphology changes to dense branching (DBM) [Fig. 2(f)]. Here, growing branches fill up the space but average density does not show periodic oscillation in the radial direction. For higher values of humidity, dehydration does not occur. In the last two morphologies, no directional variation in the intensity

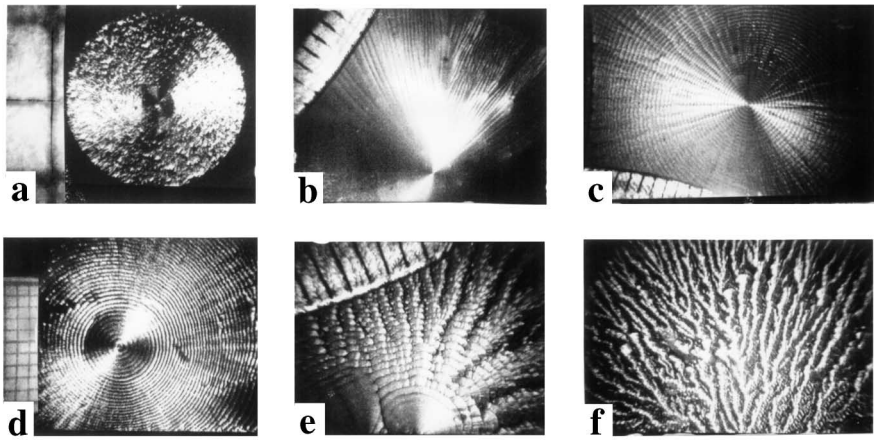

FIG. 2. Morphological variation as a function of humidity. (a) $H = 40$, nucleation for compact circular (CC) growth; (b) $H = 56$, compact radial; (c) $H = 59$, radial growth with density modulation along radius; (d) $H = 65$, density modulated circular (DMC); (e) $H = 70$, density modulated dendritic (DMD); (f) $H = 80$, dense branching morphology (DBM), arbitrary scale.

of transmitted light is observed under crossed polarizers indicating the growth to be totally amorphous. Similar morphological transitions are observed at $T = 23$, 25, and 27°C. Variation in c from $0.1M$ to $0.3M$ makes the patterns thicker. At higher temperatures, it is difficult to get a metastable solution phase. At higher c, the layer of supersaturated solution formed is very thick to merit study of 2D patterns. Dehydration does not occur at very low temperatures.

Average radius of a growing front as a function of time is measured for different morphologies (Fig. 3) using an indigenous image acquisition and analysis system. [18]. The growth is linear, indicating a constant velocity of interface propagation. The slope of the line gives the growth velocity. Growth velocity, obtained by least square fitting, increases with increasing humidity up to $H \sim 65$, beyond which it does not vary significantly though the morphologies change (Table I).

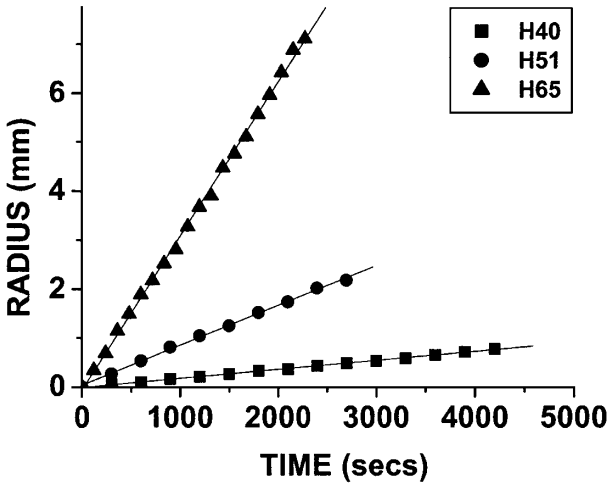

FIG. 3. Growth radius as a function of time for $H = 40$, 51, and 65.

The ring morphologies observed in these experiments are not similar to Liesegang rings. In Liesegang ring patterns, the ring radius $\sim t^{1/2}$ and the growth velocity is $\sim t^{-1/2}$. In the present system, as can be seen from Fig. 2(d), the rings are almost equally spaced, $r \sim t$ (Fig. 3), and macroscopic growth velocity is constant as a function of the radius of the growing front. This is similar to the behavior of ring patterns grown from aqueous glucose solutions [3].

In order to understand how morphological variations are induced, a simple observation is made. These solutions are inspected after the solution concentration reaches a steady state. For $H = 40$, $c_{ss} > 90$ and, if the slide is held vertical, the solution does not flow. With a little scraping, the solution can be rolled into a ball, thus indicating it to be a soft solid. This indicates that the solution is highly viscous. Thus, this is a solution in which molecular diffusion is restricted. This results in a compact circular growth [Fig. 2(a)]. For $H \sim 80$, $c_{ss} \sim 70$. If the slide is held vertical, the solution flows. This indicates that the solution is less viscous and molecular diffusion is possible. A dense branching morphology is observed at this concentration [Fig. 2(f)]. Thus, a drastic change in morphology, from a compact circular to a dense branching, occurs when a supersaturated solution changes from a highly viscous to

TABLE I. Morphology and growth velocity as a function of humidity.

Humidity (%)	Morphology	Growth velocity (μM/s)
40	Compact circular	0.18 ± 0.002
51	Compact circular	0.81 ± 0.001
65	DMC	3.13 ± 0.003
72	DMD	3.82 ± 0.02
80	DEN	2.97 ± 0.04

a less viscous medium, due to a change in humidity from 40 to 80.

A simplified picture of the growth of density modulated circular and dendritic morphologies can also be given. It is reasonable to assume that the density of precipitate, ρ_p, is higher than that of the solution, ρ_s, from which it evolves. This results in a precipitate with a radius r_p smaller than that of the solution from which it precipitates, r_s, thus leaving a gap Δ between the solution and the precipitate. Δ, and hence, the ring width increases with increasing H, that is, decreasing c_{ss}. A depletion region develops around the precipitate with concentration $c'_{ss} = c_{ss} - \delta$. For higher c_{ss}, c'_{ss} will fall in the viscous regime, and compact circular growths will occur. With decreasing c_{ss}, at some stage, c'_{ss} will fall to a value where molecular diffusion will be possible, though c_{ss} will still remain in the viscous regime. Molecules in the depletion region will diffuse to the surface of the precipitate. The precipitate will grow until the solution in the depletion region is devoid of solute particles. The next precipitation will now be on the inner periphery of the surrounding solution, thus resulting in density modulated morphologies. According to Mullins and Sekerka [19], rate of growth of a spherical harmonic distortion roughly varies as G-C, where G is related to concentration gradient and C to capillarity. It is fairly reasonable to assume that, for higher c_{ss}, Δ and δ are small and G will be suppressed resulting in a shape preserving ring morphology. When Δ and δ increase, G will increase, thus resulting in dendritic growth in the region between two rings. The origin of radial morphologies is not understood.

In conclusion, I have investigated a simple system of a dehydrating film of aqueous ascorbic acid solution which gives a sequence of morphological transitions. Novel features observed in these experiments are as follows: (1) In this system after initial loss of solvent by evaporation, a metastable supersaturated solution phase is formed, where the solution concentration remains constant over a long period of time. (2) Morphological transitions occur as a function of c_{ss}, which can be changed in a controlled manner by varying humidity. (3) Occurrence of density modulated radial and density modulated dendritic morphology is reported for the first time. (4) Morphological transitions seem to occur due to changes in several factors such as diffusion properties of the system, rate of evaporation in the depletion region, rate of precipitation, solution concentrations c_{ss} and c'_{ss}, and complex interactions between solution, solute, solvent, and the substrate. At present, the mechanism of growth of different morphologies is not clearly understood.

The author is thankful to Professor Deepak Dhar and Professor Mustansir Barma for fruitful discussions and valuable suggestions.

[1] *Fractal Growth Phenomena*, edited by T. Vicsek (World Scientific, Singapore, 1989).
[2] B. Simon and Y. Pomean, Phys. Fluids A **3**, 380 (1991).
[3] A. S. Pananjpe, Phys. Lett. A **176**, 349 (1993); Phase Transit. **64**, 115 (1998).
[4] Y. Sawada, A. Dougherty, and J. P. Gollub, Phys. Rev. Lett. **56**, 1260 (1986); D. Grier, E. Ben-Jacob, R. Clark, and L. M. Sander, Phys. Rev. Lett. **56**, 1264 (1986); F. Argoul and A. Kuhn, Physica (Amsterdam) **213A**, 209 (1995).
[5] D. A. Kessler, J. Koplik, and H. Lavine, Adv. Phys. **37**, 255 (1988); S. Roy and S. Tarafdar, Phys. Rev. E **54**, 6495 (1996).
[6] S. Bodea, L. Vignon, R. Ballou, and P. Molho, Phys. Rev. Lett. **83**, 2612 (1999).
[7] S. R. Forest and T. A. Witten, Jr., J. Phys. A **12**, L109 (1979).
[8] T. A. Witten and L. M. Sander, Phys. Rev. B **27**, 5686 (1983); T. Vicsek, Phys. Rev. Lett. **53**, 2281 (1984); P. Gerik *et al.*, Phys. Rev. A **32**, 3156 (1985).
[9] A. S. Paranjpe *et al.*, Phys. Lett. A **140**, 193 (1989); A. Kuhn, F. Argoul, J. F. Muzy, and A. Arneodo, Phys. Rev. Lett. **73**, 2998 (1994).
[10] E. Ben-Jacob *et al.*, Physica (Amsterdam) **187A**, 378 (1992); J. Wakita, I. Rafols, H. Itoh, T. Matsuyama, and M. Matsushita, J. Phys. Soc. Jpn. **67**, 3630 (1998).
[11] R. C. Brower *et al.*, Phys. Rev. A **29**, 1335 (1984); D. G. Grier *et al.*, Phys. Rev. Lett. **64** , 2152 (1990).
[12] O. Shochet and E. Ben-Jacob, Phys. Rev. E **48**, R4168 (1993).
[13] E. Ben-Jacob and P. Garik, Nature (London) **343**, 523 (1990).
[14] D. R. Link *et al.*, Phys. Rev. Lett. **84**, 5772 (2000).
[15] H. K. Henish, *Crystals in Gels and Liesegang Rings* (Cambridge University Press, Cambridge, England, 1988), pp. 121–124.
[16] H. Itoh, J. Wakita, T. Matsuyama, and M. Matsushita, J. Phys. Soc. Jpn. **68**, 1436 (1999); E. J. Dens and J. F. Van-Impe, Math. Comput. Simul. **53**, 443 (2000); M. Mimura, H. Sakaguchi, and M. Matsushita, Physica (Amsterdam) **282A**, 283 (2000).
[17] L. Zeiri, O. Younes, S. Efrima, and M. Deutsch, Phys. Rev. Lett. **79**, 4685 (1997).
[18] A. S. Paranjpe *et al.*, Indian J. Pure Appl. Phys. **35**, 316 (1997).
[19] W. W. Mullins and R. F. Sekerka, J. Appl. Phys. **34**, 323 (1963).